C. R. Palevol 14 (2015) 637–645

Contents lists available at ScienceDirect

Comptes Rendus Palevol

www.sciencedirect.com

General Palaeontology, Systematics and Evolution (Vertebrate Palaeontology)

Growth and life history of Middle Miocene deer (Mammalia, Cervidae) based on bone histology

Croissance et histoire de vie de cervidés (Mammalia, Cervidae) du Miocène moyen (Mammalia, Cervidae) : apport de l'histologie osseuse

Eli Amson , Christian Kolb , Torsten M. Scheyer , Marcelo R. Sánchez-Villagra *

Paläontologisches Institut und Museum der Universität Zürich, Karl Schmid-Strasse 4, Zürich CH-8006, Switzerland

ARTICLE INFO

Article history:
Received 21 April 2015
Accepted after revision 15 July 2015
Available online 1 October 2015

Handled by Michel Laurin

Keywords:
Bone histology
Cervidae
Dicrocerus
Euprox
Middle Miocene
Palaeohistology
Skeletochronology

ABSTRACT

Our knowledge of the histology of the Cervidae (deer) was recently expanded with a work describing long bone and tooth histology of various taxa (Kolb et al., 2015a). Included in this study was the Miocene *Procervulus*, an early cervid whose growth rate was found to be especially low. The present study examines further "stem-cervid" bone histology in describing that of other Miocene taxa, *Dicrocerus elegans* and *Euprox* sp. With their inclusion in the dataset of Kolb et al. (2015a), we estimate the ancestral growth rates among cervids, and studied its correlation with body size. The skeletochronology of *Dicrocerus* suggests a relatively high growth rate for its body size differing from the condition of *Procervulus* and *Euprox*, and hence, documenting diversity in the life history traits of Miocene cervids.

Mots clés :
Histologie osseuse
Cervidae
Dicrocerus
Euprox
Miocène moyen
Paléohistologie
Squelettochronologie

RÉSUMÉ

Notre connaissance de l'histologie des Cervidae a récemment été étendue grâce à une étude décrivant l'histologie osseuse et dentaire chez divers taxons (Kolb et al., 2015a). Cette précédente étude présentait *Procervulus*, un cervidé miocène dont le taux de croissance a été caractérisé comme particulièrement bas. Nous décrivons ici l'histologie osseuse de deux autres « stem-cervidés » miocènes, *Dicrocerus elegans* et *Euprox* sp. En les incorporant dans le jeu de données de Kolb et al. (2015a), nous estimons le taux de croissance ancestral au sein des cervidés, et étudions sa corrélation avec la taille corporelle. Les données squelettochronologiques chez *Dicrocerus* indiquent un taux de croissance relativement fort pour sa taille corporelle, contrastant avec ceux de *Procervulus* et *Euprox*, et documentant donc une diversité de traits d'histoire de vie chez les cervidés miocènes.

* Corresponding author.
E-mail address: m.sanchez@pim.uzh.ch (M.R. Sánchez-Villagra).

http://dx.doi.org/10.1016/j.crpv.2015.07.001
1631-0683/

1. Introduction

The investigation of the palaeobiology of "stem-cervids" from the Miocene is necessary to understand the origin of the diverse life histories of deer. *Dicrocerus elegans* Lartet 1837, one of these early cervids (Azanza, 1993; Gentry, 1994), was originally described from the French locality of Sansan (local Helvetian age), which corresponds to the mammalian Neogene age MN6 [Middle Miocene, Langhian, *ca.* 15 Ma; (Peigné and Sen, 2012)]. *Dicrocerus*, of relatively intermediate body size [*ca.* 50 kg; (Costeur et al., 2012)], is characterized by its long pedicle and bifid "protoantler". It is known from numerous specimens, which have allowed, for instance, to propose that the female of *Dicrocerus*, like the extant *Rangifer* (Reindeer), were antlered, and that the species was marked by sexual dimorphism regarding size and shape of the antlers (Ginsburg and Azanza, 1991). However, different ontogenetic stages have been suggested as an alternative explanation (Gentry et al., 1999). The growth cycle of the "protoantler" comprises a shedding phase of the velvet-like skin and a phase with bare and dead bone tissue before casting (Azanza et al., 2012). Such a cycle appears to be an apomorphic feature grouping *Dicrocerus* with later cervids. However, the protoantlers of *Dicrocerus*, growing over a longer period than the annually deciduous antlers, may represent the ancestral condition for later cervids (DeMiguel et al., 2014). Although brachydont, *Dicrocerus* is considered to be a mixed feeder (Solounias and Moelleken, 1994).

Euprox is another cervid from the Middle Miocene of Europe (Gentry et al., 1999). Little is known about *Euprox*, hypothesized to be sister-taxon of other Muntiacini (Azanza, 1993), albeit this is controversial (Gentry et al., 1999).

Procervulus praelucidus (Obergfell 1957), known from the Early Miocene [MN3, Ginsburg (2011)], is regarded as being, with the rest of the Procervulinae, sister-group of all other cervids, including *Dicrocerus* (Azanza, 1993). This species was recently included in a study of long bone and dental histology concerned with cervids life history evolution in order to estimate skeletal maturity and growth rate (Kolb et al., 2015a). *Procervulus* distinguished itself in featuring the lowest estimated growth rate of all the cervids sampled in that study. We here investigate if such a condition is widespread in "stem-cervids". The bone histology and skeletochronology of *Dicrocerus* and *Euprox* will hence be investigated here to gain insight into life history traits in early cervids, as it was previously performed regarding feeding styles (DeMiguel et al., 2008).

2. Material and methods

For *Dicrocerus elegans*, eleven bones, comprising three humeri (MNHN.F.Sa7330, Sa7341, and Sa7343), three radii (MNHN.F.Sa2453, Sa2470, and Sa7063), two femora (MNHN.F.Sa6877, Sa6889), and three tibiae (MNHN.F.Sa6910, Sa6917, and Sa8163), were sampled. As indicated by epiphyseal closure, the specimens correspond to subadult to adult individuals. For *Euprox* sp., one femur from the locality of Steinheim (Germany), with epiphyseal lines still slightly visible, was sampled (NMB Sth.1281). Thin-sections were prepared following conventional procedure (Chinsamy-Turan, 2005; Kolb et al., 2015a; Padian and Lamm, 2013). The sections were taken as close as possible from the mid-diaphyseal level (see Appendix A for estimation of relative position of each thin-section). Observations were performed with a petrographic microscope (Leica DM 2500M®) under normal transmitted or cross-polarized light, in some cases with the use of a lambda compensator. Photographs were taken with a digital camera (Leica DFC 420C®) installed on the microscope. The quantification of the growth rate [annual growth rate with an estimated mean growth period of 260 days, as explained in Kolb et al. (2015a), and based on Köhler et al. (2012)], was performed following published methodology (Kolb et al., 2015a), using the Leica IM 50 Image Manager® software. Only the growth rate of the femur and tibia will be discussed, because these bones were considered by Kolb et al. (2015a) as the most informative. The growth zone measurements were taken in the anterior region of the bones, in order to be consistent with the data from Kolb et al. (2015a). The histological terminology follows Francillon-Vieillot et al. (1990). Regarding the definition of the OCL (necessary for the skeletal maturity estimation), we follow Ponton et al. (2004) in acknowledging its presence when parallel-fibred/lamellar and avascular tissue forms the external-most region of the cortex.

A timetree was used to perform phylogenetically-informed statistical tests. The relationships and divergence times in extant taxa are based on Hassanin et al. (2012). Regarding relationships and divergence times of extinct taxa, the following data were used (and see above for *Dicrocerus* and *Procervulus*). Megacerina *sensu* Vislobokova (2013) are here represented by the giant *Megaloceros giganteus* and *Sinomegaceros yabei*. *M. giganteus* is known from 0.4 Ma to 6 900 years BP (Stuart et al., 2004). The sampled specimen of *S. yabei* (OMNH QV-4067) comes from the Late Pleistocene (ca. 20–30,000 years) of Japan (Kolb et al., 2015b). Closely related to the Megacerina, the dwarf *Candiacervus* from Crete was also included (we consider the Megacerina to be included, along with *Candiacervus*, *Dama dama*, the Fallow deer, and *Cervus elaphus*, the Red deer, into the Cervini). Specimens of *C. ropalophorus* are known to be at least 43,600 years old in one locality, and dated at *ca.* 21,500 years in another (Vislobokova, 2013). *Candiacervus* sp. II is also well known from the Late Pleistocene (Van Der Geer et al., 2010, p. 333). The relationships among Megacerina, *Candiacervus*, and with their closest extant relative, *Dama* (Lister et al., 2005), are not well understood (A.M. Lister, pers. comm.). We hence prefer to leave a polytomy in the topology. The divergence times within the (Megacerina + *Candiacervus* + *Dama*) clade are based on Vislobokova (2013). Due to the age of the Megacerina fossils, the origin of the Cervini clade was pushed back when compared to the molecular dating of Hassanin et al. (2012). Since *Euprox* is found in MN6 (Gentry et al., 1999) and is hypothesized as sister-taxon of other Muntiacini (Azanza, 1993), the origins of Cervinae and crown-Cervidae were pushed back as well. However, this hypothesis should be treated with caution, because the phylogenetic position of *Euprox* is regarded as controversial (Gentry et al., 1999). A nexus file containing the timetree is given as Appendix A.

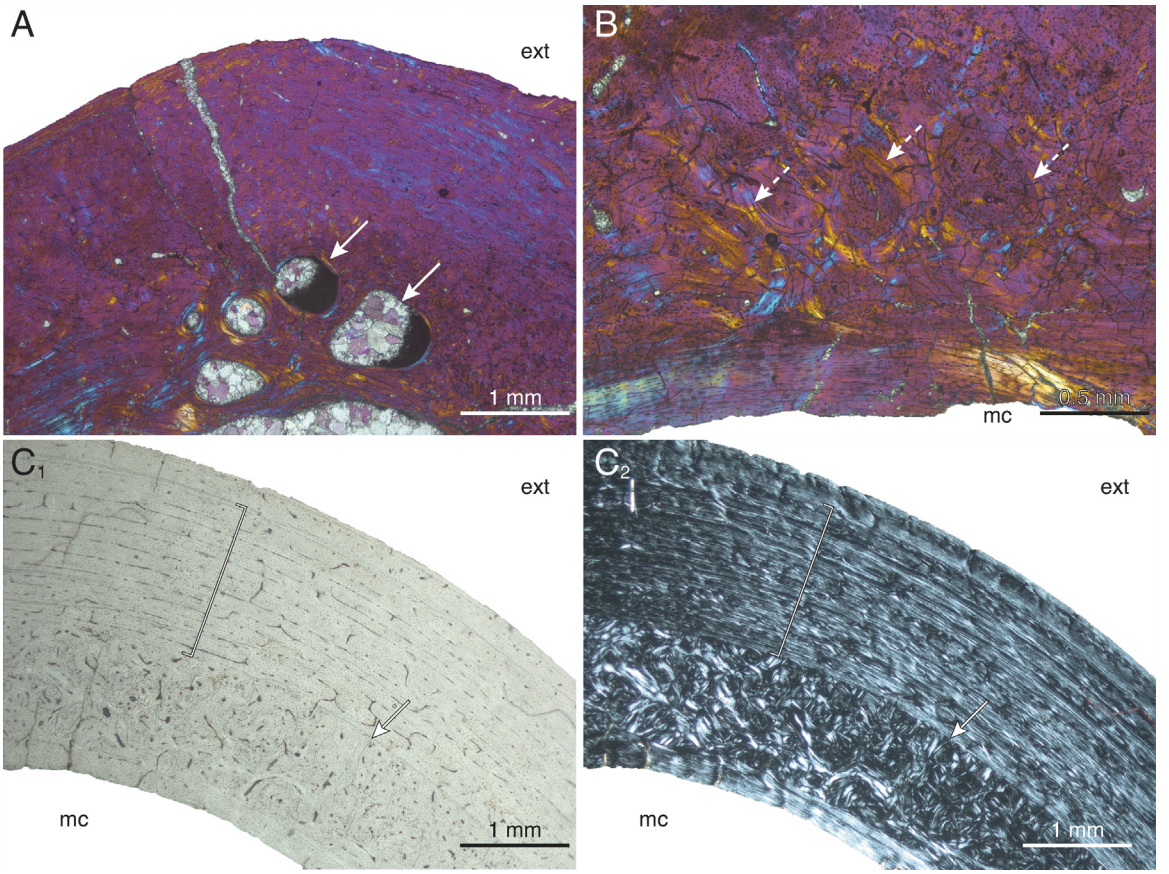

Fig. 1. (Color online). Histological features of the humerus of *Dicrocerus elegans*. A. Large resorption vacuities (white continuous arrows) seen under CPL-λ (anterior region; MNHN.F.Sa.7341). B. Secondary osteons of various orientations describing pseudo-circular patterns (white dashed arrows), seen under CPL-λ (anteromedial region; MNHN.F.Sa.7341). C. Fibrolamellar tissue (with a very low amount of fibrous tissue) with laminar to plexiform vascularization (white with black outline bracket) seen under NL (C_1) and CPL (C_2) (posterolateral region; MNHN.F.Sa.7343). Note the presence of a LAG (white with black outline continuous arrows) that sharply defines externally a strongly remodeled zone. Abbreviations: ext, exterior; mc, medullary cavity.
Fig. 1. (Couleur en ligne). Caractéristiques histologiques de l'humérus chez *Dicrocerus elegans*. A. Grandes cavités de résorption (flèches blanches en trait plein) vues sous CPL-λ (région antérieure; MNHN.F.Sa.7341). B. Ostéones secondaires d'orientations diverses formant des motifs pseudo-circulaires (flèches blanches en trait pointillé), observées sous CPL-λ (région antéromédiale; MNHN.F.Sa.7341). C. Tissu fibrolamellaire (à faible teneur en os fibreux) à vascularisation laminaire à plexiforme (crochet blanc à contour noir), observé sous NL (C_1) et CPL (C_2) (région postérolatérale; MNHN.F.Sa.7343). Noter la présence d'une LAG définissant nettement la limite externe d'une zone fortement remaniée. Abréviations : ext, extérieur ; mc, cavité médullaire.

A test for the presence of phylogenetic signal was performed for the growth rates and body size proxy (anteroposterior diameter of the section) using the Mesquite software (Maddison and Maddison, 2011) and a previously published procedure (Laurin, 2004; Quemeneur et al., 2013). It consists of the comparison of the squared length of the reconstructed parameter to those of 10,000 trees in which the terminal taxa were randomly reshuffled. The *P*-value of this test will be the number of trees (divided by 10,000) shorter than the initial tree. The ancestral character values were reconstructed using squared-change parsimony in Mesquite. The phylogenetically-informed linear regression of the growth rate against anteroposterior diameter of the section was performed using phylogenetically independent contrasts (PIC) analysis with the Mesquite software and its PDAP:PDTREE module (Midford et al., 2011).

Institutional abbreviations:

NMB, Naturhistorisches Museum Basel, Switzerland; **MNHN**, Muséum national d'Histoire naturelle, Paris, France; **OMNH**, Osaka Museum of Natural History, Japan; **ZIUK**, Zoologisches Institut der Universität Kiel, Germany.

Other abbreviations:

CPL, crossed polarized light; **CPL-λ**, crossed polarized light with the addition of a lambda compensator; **NL**, natural light; **OCL**, outer circumferential layer

3. Histological description

All sampled bones feature a free medullary cavity and a compact cortex. Except for a few minor instances, trabecular bone was not observed.

3.1. *Humerus of* Dicrocerus

A layer of endosteal lamellar bone of variable thickness is found on the whole circumference of the innermost cortex. Most of the inner region of the rest of the cortex is heavily remodeled in all three specimens, preventing

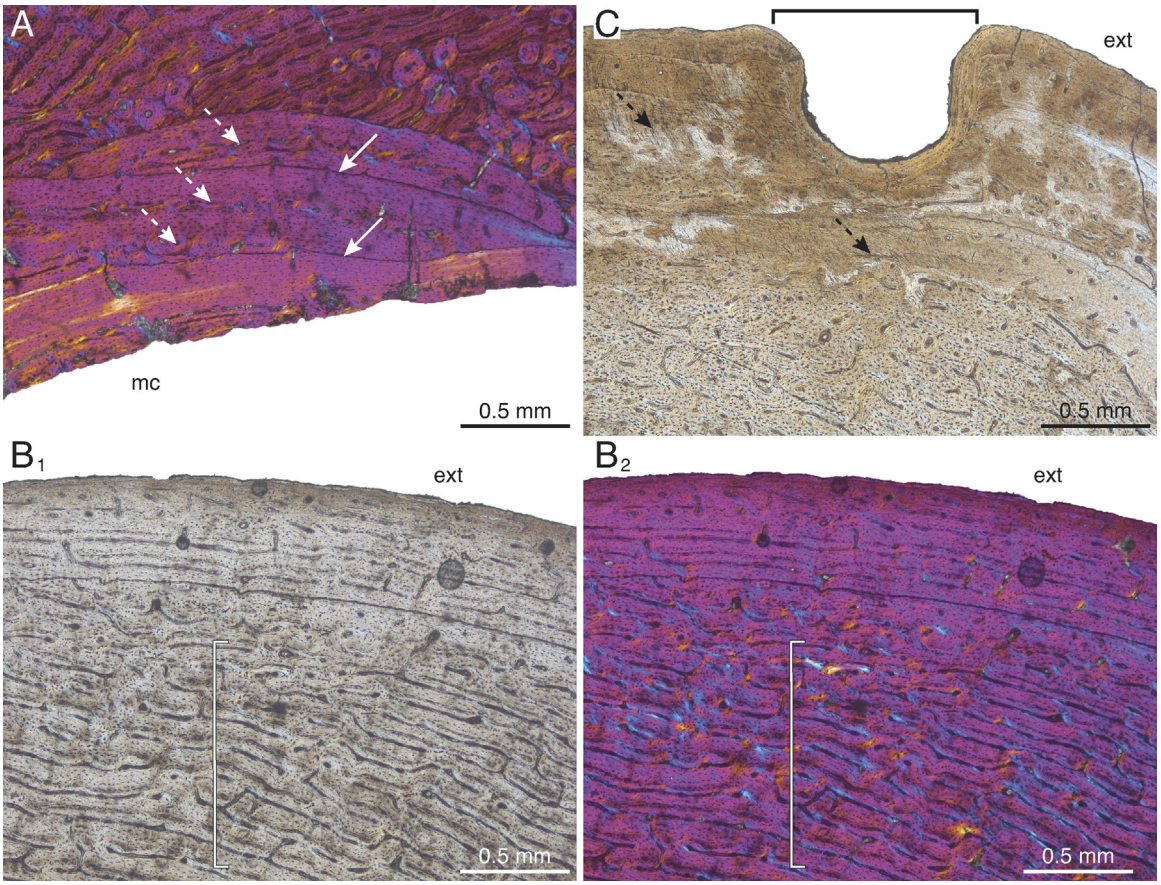

Fig. 2. (Color online). Histological features of the radius of *Dicrocerus elegans*. A. Lamellar endosteal deposit featuring cement lines (white continuous arrows) and vascular canals (white dashed arrows), seen under CPL-λ (anterolateral region; MNHN.F.Sa2470). B. Central region of the cortex formed by fibrolamellar bone with a plexiform to reticular vascularization (white with black outline bracket), seen under NL (B_1) and CPL-λ (B_2) (medial region; MNHN.F.Sa2470). C. Outer nutrient foramen (black bracket) with numerous Sharpey's fibre bundles (black dashed arrows), seen under NL (posterolateral region; MNHN.F.Sa7063). Abbreviations: ext, exterior; mc, medullary cavity.

Fig. 2. (Couleur en ligne). Caractéristiques histologiques du radius chez *Dicrocerus elegans*. A. Dépôt lamellaire endostéal présentant lignes cimentantes (flèches blanches en trait plein) et canaux vasculaires (flèches blanches en trait pointillé), observés sous CPL-λ (région antérolatérale; MNHN.F.Sa2470). B. Région centrale du cortex formée par de l'os fibrolamellaire à vascularisation plexiforme à réticulée (crochet blanc à contour noir), observée sous NL (B_1) et CPL-λ (B_2) (région médiale; MNHN.F.Sa2470). C. Foramen nourricier externe (crochet noir) cerné de nombreux paquets de fibres de Sharpey (flèches noires en trait pointillé). Abréviations : ext, extérieur ; mc, cavité médullaire.

the description of the primary structures. In one specimen (MNHN.F.Sa7341) large resorption vacuities, most likely related to a bone drift process, can be noted (Fig. 1A). These vacuities are surrounded by lamellar bone. The middle region of the cortex is either remodeled by longitudinal, oblique, and transverse secondary osteons (MNHN.F.Sa7330, MNHN.F.Sa7341, and part of MNHN.F.Sa7343) that can describe in some places pseudo-circular patterns (Fig. 1B), or be formed by fibrolamellar tissue, and with laminar to plexiform vascularization (Fig. 1C). In the outermost cortex, the vascularization is usually reduced to a few longitudinal vascular canals, and a clear OCL is found on two of the three specimens (MNHN.F.Sa7330; MNHN.F.Sa7341). Two specimens (MNHN.F.Sa7341 and MNHN.F.Sa7343) show a peculiar pattern of remodeling, in which most of the secondary osteons are restricted and almost entirely forming an area sharply defined externally by a line of arrested growth (LAG) (Fig. 1C).

3.2. *Radius of* Dicrocerus

In this bone, and when present, the endosteal deposit has a particularly irregular thickness, with sometimes several cement lines ("cementing line" *sensu* Francillon-Vieillot et al. (1990); Fig. 2A) and few longitudinal vascular canals. The rest of the cortex, either partially or entirely remodeled, is formed by fibrolamellar bone with a plexiform or reticular vascularization (Fig. 2B), and becomes poorly vascularized outwardly. One specimen (MNHN.F.Sa7063) corresponds to a section at the level of the outer nutrient foramen, as shown by the presence of a concavity in its posterolateral region. Numerous Sharpey's

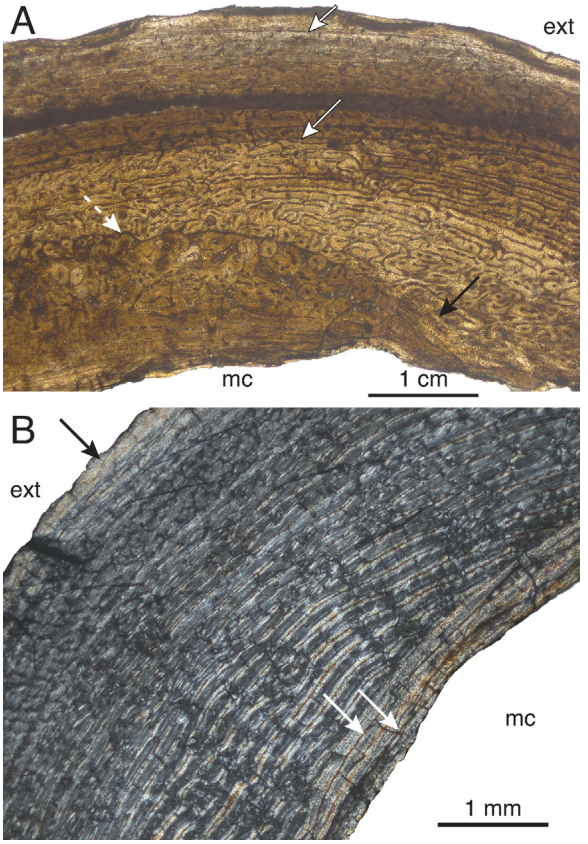

Fig. 3. (Color online). Histological features of the femur of *Dicrocerus elegans* and *Euprox* sp. A. Anterior region of *Dicrocerus elegans* (MNHN.F.Sa6877) seen under NL. Note the presence of a resorption line within the cortex (white dashed arrow) that is not found throughout the section, as shown by the presence of primary bone where it would have been found (black arrow); note also the two first LAGs (white with black outline continuous arrows; the first is a double LAG) delimiting the second growth zone. B. Anterior region of *Euprox* (NMB Sth.1281) seen under CPL. Note the cement lines in the endosteal deposit (white arrows), and a thin layer in the external-most cortex formed by lamellar bone (highly birefringent) without vascularization (black arrow). Abbreviations: ext, exterior; mc, medullary cavity.

Fig. 3. (Couleur en ligne). Caractéristiques histologiques du fémur de *Dicrocerus elegans* et *Euprox* sp. A. Région antérieure chez *Dicrocerus elegans* (MNHN.F.Sa6877), observée sous NL. Noter la présence d'une ligne de résorption au sein du cortex (flèche blanche en trait pointillé), qui n'est pas présente sur toute section, comme indiqué par la présence de tissu primaire (flèche noire) ; noter aussi les deux premières LAGs (flèches blanches en trait plein à contour noir) définissant la seconde zone de croissance. B. Région antérieure chez *Euprox* (NMB Sth. 1281), observée sous CPL. Noter la présence de lignes cimentantes dans le dépôt endostéal (flèches blanches) et celle, dans la région la plus externe du cortex, d'un fin dépôt formé par de l'os lamellaire sans vascularisation (flèche noire). Abréviations : ext, extérieur ; mc, cavité médullaire.

fibre bundles are seen in its vicinity (Fig. 2C). None of the specimens features a clear OCL.

3.3. *Femur of* Dicrocerus

A very narrow to absent layer of endosteal bone is observed. The middle part of the cortex is well remodeled in both available specimens. The secondary osteons are longitudinal and to a lesser extent oblique, and in some places describe pseudo-circular patterns. In the inner part of lateral region of MNHN.F.Sa6889, remnants of trabeculae are present. Where not entirely remodeled (especially in MNHN.F.Sa6889), the outermost cortex is weakly vascularized, with few, mostly longitudinal, vascular canals, and mainly consists of lamellar bone. One specimen (MNHN.F.Sa6877) shows a cement line that cannot be interpreted as a LAG, due to its irregular and wavy shape and because it is not present throughout the whole section (Fig. 3A). Based on a similar structure described by Klevezal (1996, fig. 9), we tentatively interpret it as a resorption line. Neither of the specimens features an OCL.

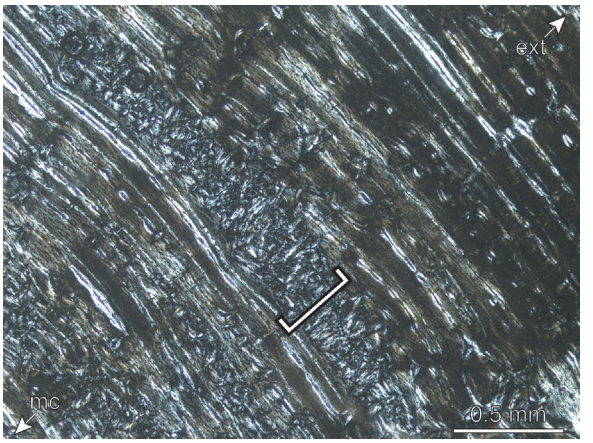

Fig. 4. (Color online). Histological features of the tibia of *Dicrocerus elegans*. Detail of a zone with reticular vascularization (white with black outline bracket) between laminae of the main plexiform vascularization, under CPL (posterior region; MNHN.F.Sa6910). Abbreviations: ext, exterior; mc, medullary cavity.

Fig. 4. (Couleur en ligne). Caractéristiques histologiques du tibia chez *Dicrocerus elegans*. Détail d'une zone à vascularisation réticulée (crochet blanc à contour noir) intercalée entre les lamines de vascularisation plexiforme principale, observée sous CPL (région postérieure, MNHN.F.Sa6910). Abréviations : ext, extérieur ; mc, cavité médullaire.

3.4. *Femur of* Euprox

Although rather thin, the layer of endosteal bone in the sampled specimen of *Euprox* sp. (NMB Sth.1281) features two cement lines (Fig. 3B). The cortex is mostly formed by plexiform fibrolamellar bone with a high amount of fibrous tissue. Externally the vascularization becomes reticular and is less present. Secondary osteons are extremely scarce. The external-most cortex is mostly formed by lamellar bone and does not show any vascularization (Fig. 3B). However, this concerns a very thin layer of bone, which prevents from securely recognizing an OCL.

3.5. *Tibia of* Dicrocerus

An endosteal lamellar layer of irregular thickness is found in all specimens. Most of the cortex is formed by fibrolamellar plexiform bone. Reticular vascularization is also observed, sometimes forming lenticular areas between laminae of the plexiform vascularization (Fig. 4). The outermost cortex is formed by avascular lamellar bone. The secondary osteons have a longitudinal, oblique, or radial

Table 1
Zone measurements and associated growth rates in the anterior region of long bones of *Dicrocerus elegans* and *Euprox* sp.
Tableau 1
Mesures des zones et taux de croissance associés dans la région antérieure des os longs chez *Dicrocerus elegans* et *Euprox* sp.

		LAG count	GZ number	GZ thickness (mm)	Mean GZ (mm/a)	Mean GR (μm/d) 260 d
Dicrocerus elegans						
Femur	MNHN.F.Sa6877	2 (2)	2nd	0.98	0.98	3.77
Tibia	MNHN.F.Sa6910	4 (4)	2nd	1.57	1.36	5.21
			3rd	0.20	0.20	0.77
			4th	0.12	0.12	0.46
	MNHN.F.Sa6917	2 (6)	2nd	1.14		
	MNHN.F.Sa8163	1 (5)		–		
Humerus	MNHN.F.Sa7330	4 (7)	2nd	0.44	1.14	1.69
			3rd	0.17	0.25	0.65
			4th	0.06		0.23
	MNHN.F.Sa7343	3 (4)	2nd	1.84		7.08
			3rd	0.33		1.27
Radius	MNHN.F.Sa2453	2 (2)	2nd	0.44		1.69
	MNHN.F.Sa2470	2 (2)	2nd	0.65		2.50
	MNHN.F.Sa7063	3 (3)	2nd	0.28		1.08
			3rd	0.08		0.31
***Euprox* sp.**						
Femur	NMB Sth.1281	2 (2)	2nd	0.47		1.81

d: days; **GR**: growth rate; **GZ**: growth zone; **LAG**: line of arrested growth in the anterior region of the bone used for the growth zone measurements and, between brackets, maximum number of LAGs found on the section.

orientation. The available specimens are weakly remodeled, with secondary osteons restricted to the inner half of the cortex. One specimen (MNHN.F.Sa6917) features an external deposit of avascular lamellar bone, but it is too thin to securely recognize it as an OCL.

4. Skeletochronology

When not obscured by secondary remodeling (especially the case in the sections farther away from the midshaft), all sampled bones feature at least one identifiable LAG. The LAG counts for each specimen (of which the count is not prevented by remodeling) are listed in Table 1. In *Dicrocerus*, for one specimen (MNHN.F.Sa7330; humerus) it was possible to conduct an estimation of skeletal maturity, thanks to its preservation of LAGs that are not obscured by secondary remodeling and of a clear OCL (Fig. 5). No LAG is lost (resorbed) during ontogeny in the femur and tibia of cervids (Kolb et al., 2015a). Based on the generally similar histomorphological pattern, it is also likely the case in the humerus and radius. With a count of five LAGs before the OCL, we hence hypothesize that the skeletal maturity in *Dicrocerus* was reached after five years. More specimens are required to make such an assertion for *Euprox* sp., because it was not possible to securely recognize an OCL in the available specimen.

The thickness of all zones and associated growth rates are given in Table 1. In *Dicrocerus*, and for the femur, only the second growth zone (between the first two LAGs) of one specimen could be measured (Fig. 3A). Being 0.98 mm thick, it corresponds to an annual growth rate of 3.77 μm per day. For the tibia, we were able to measure the thickness of the second growth zone on two specimens; in one of those specimens, we were also able to measure that of the second and third zones. The mean value of annual growth rate for the first three zones in the tibia is of 2.15 μm per day. In

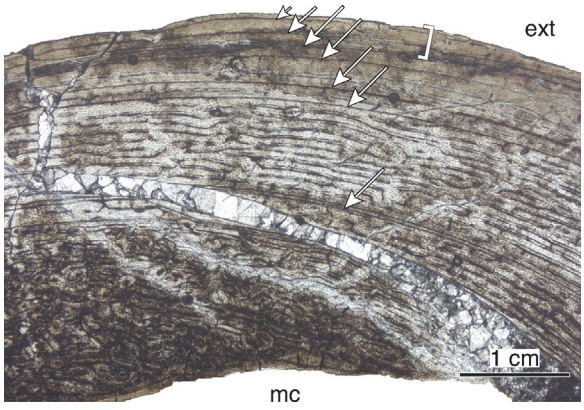

Fig. 5. (Color online). Seven lines of arrested growth (LAGs; indicated by arrows) and the OCL (outer circumferential layer; indicated by bracket) in the medial region of a humerus of *Dicrocerus elegans* (MNHN.F.Sa7330).
Fig. 5. (Couleur en ligne). Sept lignes d'arrêt de croissance (indiquées par des flèches) et l'OCL (système fondamental externe; indiqué par un crochet) dans la région médiale d'un humérus de *Dicrocerus elegans* (MNHN.F.Sa7330).

Euprox, the sampled femur yielded the first two LAGs defining a second growth zone that is 0.47 mm thick (Fig. 3B). This corresponds to an annual growth rate of 1.81 μm per day.

5. Discussion and conclusions

The free medullary cavity and compact cortex is a feature common to all cervids and more generally to most terrestrial amniotes (Laurin et al., 2011). The bone histology of *Dicrocerus* is on the whole consistent with that of other small to medium-sized cervids (Kolb et al., 2015a). Indeed, the primary bone tissue is mostly fibrolamellar and highly vascularized in the inner and middle cortex, with a mostly plexiform pattern, and the outer cortex is weakly

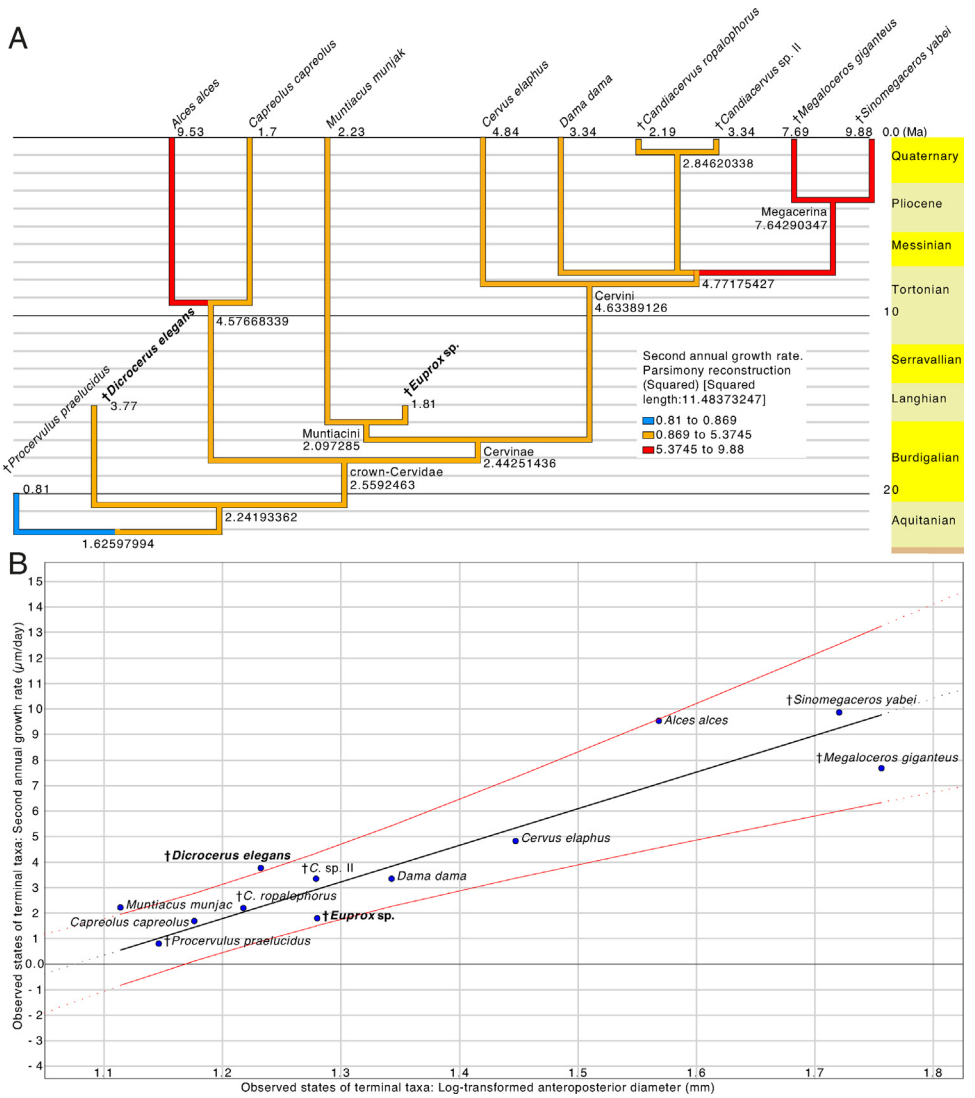

Fig. 6. (Color online). Phylogenetically-informed analysis of the relationship between femoral growth rate and body size in cervids. A. Timetree on which the second annual growth rate (260 days of growth) is mapped with Mesquite (Maddison and Maddison, 2011) and its stratigraphic tools module (Josse et al., 2006). The ancestral character states were reconstructed using squared-change parsimony. B. Independent contrasts least-squares linear regression (black line) of the second annual growth rate against the anteroposterior diameter of the section (body size proxy) mapped onto the original tip data space, performed with the PDAP:PDTREE module (Midford et al., 2011) of Mesquite. The red lines (see online version) represent the 95% confidence interval.
Fig. 6. (Couleur en ligne). Analyse prenant en compte la phylogénie de la relation entre le taux de croissance fémoral annuel et la taille corporelle chez les cervidés. A. Arbre phylogénétique calibré dans le temps, sur lequel le taux de croissance annuel (260 jours de croissance) de la deuxième année est plaqué grâce à Mesquite (Maddison et Maddison, 2011) et son module d'outils stratigraphiques (Josse et al., 2006). Les valeurs ancestrales ont été reconstruites grâce à l'algorithme de parcimonie (moindres carrés). B. Régression par méthode des moindres carrés des contrastes indépendants (droite noire) du taux de croissance annuel de la deuxième année sur le diamètre antéropostérieur de la section (proxy pour la masse corporelle) plaqué sur l'espace de données des branches terminales initiales, effectuée avec le module PDAP:PDTREE (Midford et al., 2011) de Mesquite. Les courbes rouges (voir la version en ligne) représentent l'intervalle de confiance à 95 %.

vascularized and formed by lamellar bone. The skeletal maturity, estimated in *Dicrocerus* to be reached after five years (during the sixth year of life), is reminiscent of that of *Cervus elaphus* (5-6 years old), *Megaloceros* (5–6 years old), and *Candiacervus* (5–7 years old; Kolb et al., 2015a).

The newly measured growth rates of *Dicrocerus* and *Euprox* were added to the dataset of Kolb et al. (2015a) in order to discuss them in the broader context of the Cervidae. A significant phylogenetic signal was found for the anteroposterior diameter of the section (P-value = 0.0163). For the second annual growth rate, a P-value of 0.0746 was obtained. Even though this is higher than the usual 5% threshold, we consider it as indicative of a pattern of biological significance. It should be noted that this value is at least partly explained by the fact that a high growth rate was independently acquired in *Alces*, the Elk, and the Megacerina clade (Fig. 6A). As a matter of fact, pruning *Alces* from the tree brings the P-value of this test to 0.0286. Furthermore, a phylogenetically-informed linear regression was performed. After trying all combination of

log-transformation for each variable, the untransformed growth rate against log-transformed anteroposterior bone diameter obtained the greatest correlation coefficient ($R = 0.87$). Since a phylogenetic signal is also significantly present in the log-transformed anteroposterior bone diameter (P-value < 0.01), we used it for the rest of the analysis. The absence of significant correlation for both the growth rate and the log-transformed anteroposterior bone diameter in all diagnostic checks (absolute values of standardized contrasts against their standard deviations, or against their estimated nodal values, or against the heights of their base nodes, or the estimated nodal values against heights of the base nodes of the contrasts) allowed us to perform the PIC analysis (Midford et al., 2011). With a R^2 of 0.75 and a P-value lower than 0.0004, we find that the growth rate in cervids is strongly correlated with body size (Fig. 6B), confirming the results of Kolb et al. (2015a).

The growth rate corresponding to the femoral second zone is, in *Dicrocerus* (3.77 μm/day), close to that of *Dama* and *Candiacervus* sp. II (both at 3.34 μm/day), much lower than the large-sized *Megaloceros* (7.69 μm/day), *Sinomegaceros* (9.88 μm/day), and *Alces* (9.53 μm/day). However, *Dicrocerus* features a much greater second annual growth rate than *Procervulus* (0.81 μm/day) and *Euprox* sp. (1.81 μm/day). *Dicrocerus* falls slightly above the 95% confidence interval of the phylogenetically correct linear regression (Fig. 6B), indicating a relatively high growth rate for its size. The ancestral value reconstructed for all cervids is 1.63 μm/day (Fig. 6A). The ancestral state for the *Dicrocerus* plus crown-cervids clade is 2.24 μm/day, which is already much higher than that of the Early Miocene *Procervulus* and closer to that of *Dicrocerus*, and which will be roughly found as the ancestral value for the crown-cervids, the Muntiacini (here represented by *Muntiacus* and the Middle Miocene *Euprox*), and the Cervinae as well. A first departure from this value is found at the origin of the Capreolinae, here represented by *Alces* and *Capreolus capreolus* (Roe deer). But this result is likely an artefact, as *Alces*, much larger than *Capreolus*, was shown to lower the significance of the statistical test (see above). The increase of growth rate is more probably acquired in a more restricted taxon, and sampling extinct Alcini would clarify this question. A more documented increase of growth rate is found for the Cervini, with an ancestral growth rate of 4.63 μm/day. While the relationships between *Dama*, *Candiacervus*, and the large-sized Megacerina were left as unresolved, it can be emphasized that a reversion to a lower growth rate is found in *Candiacervus* (ancestral value for the genus of 2.85 μm/day), and a steep increase is found as the ancestral value for Megacerina, with a growth rate of 7.64 μm/day.

The bone histology of *Dicrocerus* is reminiscent of those of other small to medium-sized deer. The skeletochronological data suggest that *Dicrocerus* featured a higher growth rate than the other "stem-cervid" *Procervulus* and than the Middle Miocene *Euprox*. While growth rate was shown to be strongly correlated to body size, that of *Dicrocerus* was found as particularly high (slightly above the confidence interval of the phylogenetically-informed regression), documenting diversity in the early evolution of life history traits of the Cervidae.

Acknowledgements

Christine Argot (MNHN), Loïc Costeur (NMB), and Shoji Hayashi and Hiroyuki Taruno (Osaka Museum of Natural History) are warmly thanked for granting access to the collections under their care and for their assistance. We thank Sergio Soares for his preliminary work on the *Dicrocerus* material. Finally, Loïc Costeur, Grégoire Métais, and a third anonymous reviewer are acknowledged, as well as the editor, Michel Laurin, for the improvement they brought the manuscript. This work was supported by Swiss National Fund SNF 31003A_149605 to M. R. Sánchez-Villagra and 31003A_149506 to T. M. Scheyer.

Appendix A. Supplementary data

Supplementary data associated with this article can be found, in the online version, at http://dx.doi.org/10.1016/j.crpv.2015.07.001.

References

Azanza, B., 1993. Sur la nature des appendices frontaux des cervidés (Artiodactyla, Mammalia) du Miocène inférieur et moyen. Remarques sur leur systématique et leur phylogénie. C. R. Acad. Sci. Paris, Ser. II 316, 1163–1169.

Azanza, B., DeMiguel, D., Andrés, M., 2012. The antler-like appendages of the primitive deer *Dicrocerus elegans*: morphology, growth cycle, ontogeny, and sexual dimorphism. Estud. Geol. 67, 579–602.

Chinsamy-Turan, A., 2005. The Microstructure of Dinosaur Bone: Deciphering Biology with Fine-scale Techniques. Hopkins University Press, Baltimore.

Costeur, L., Guérin, C., Maridet, O., 2012. Paléoécologie et paléoenvironnement du site miocène de Sansan. In: Mammifères de Sansan. Mem. Muséum National d'Histoire Naturelle, pp. 661–693.

DeMiguel, D., Azanza, B., Morales, J., 2014. Key innovations in ruminant evolution: a paleontological perspective. Integr. Zool. 9, 412–433.

DeMiguel, D., Fortelius, M., Azanza, B., Morales, J., 2008. Ancestral feeding state of ruminants reconsidered: earliest grazing adaptation claims a mixed condition for Cervidae. BMC Evol. Biol. 8, 13.

Francillon-Vieillot, H., Buffrénil, V., de Castanet, J., Géraudie, J., Meunier, F.J., Sire, J.-Y., Zylberberg, L., de Ricqlès, A., 1990. Microstructure and mineralization of vertebrate skeletal tissues. In: Carter, J.G. (Ed.), Skeletal Biomineralization: Patterns. Processes and Evolutionary Trends, 1. Van Nostrand Reinhold, New York, pp. 471–530.

Gentry, A.W., 1994. The Miocene differentiation of old world Pecora (Mammalia). Hist. Biol. 7, 115–158.

Gentry, A.W., Rössner, G.E., Heizmann, E.P.J., 1999. Suborder Ruminantia. In: Rössner, G.E., Heissig, K. (Eds.), The Miocene Land Mammals of Europe. Verlag Dr. Friedrich Pfeil, München, pp. 225–258.

Ginsburg, L., 2011. The Early Burdigalian (MN3; Miocene) large mammals from Estrepouy (Aquitaine basin, France): an updated faunal list. Estud. Geol. 67, 411–417.

Ginsburg, L., Azanza, B., 1991. Présence de bois chez les femelles du cervidé miocène *Dicrocerus elegans* et remarques sur le problème de l'origine du dimorphisme sexuel sur les appendices frontaux des Cervidés. C.R. Acad. Sci. Paris Ser.II 213, 121–126.

Hassanin, A., Delsuc, F., Ropiquet, A., Hammer, C., Jansen Van Vuuren, B., Matthee, C., Ruiz-Garcia, M., Catzeflis, F., Areskoug, V., Nguyen, T.T., Couloux, A., 2012. Pattern and timing of diversification of Cetartiodactyla (Mammalia, Laurasiatheria), as revealed by a comprehensive analysis of mitochondrial genomes. C.R. Biologies 335, 32–50.

Josse, S., Moreau, T., Laurin, M., 2006. Stratigraphic tools for Mesquite. http://mesquiteproject.org/packages/stratigraphicTools/.

Klevezal, G.A., 1996. Recording Structures of Mammals. Determination of Age and Reconstruction of Life History. Balkema Publishers, Rotterdam.

Kolb, C., Scheyer, T.M., Lister, A.M., Azorit, C., de Vos, J., Schlingemann, M.A., Rössner, G.E., Monaghan, N.T., Sánchez-Villagra, M.R., 2015a. Growth in fossil and extant deer and implications for body size and life history evolution. BMC Evol. Biol. 15, 1–15.

Kolb, C., Scheyer, T.M., Veitschegger, K., Forasiepi, A.M., Amson, E., van der Geer, A., Hayashi, S., van den Hoek Ostende, L.W., Sánchez-Villagra,

M.R., 2015b. Mammalian bone palaeohistology: new data and a survey. PeerJ Prepr. 3, e1405.
Köhler, M., Marín-Moratalla, N., Jordana, X., Aanes, R., 2012. Seasonal bone growth and physiology in endotherms shed light on dinosaur physiology. Nature 487, 358–361.
Laurin, M., 2004. The evolution of body size. Cope's rule and the origin of amniotes. Syst. Biol. 53, 594–622.
Laurin, M., Canoville, A., Germain, D., 2011. Bone microanatomy and lifestyle: a descriptive approach. C. R. Palevol 10, 381–402.
Lister, A.M., Edwards, C.J., Nock, D.A.W., Bunce, M., van Pijlen, I.A., Bradley, D.G., Thomas, M.G., Barnes, I., 2005. The phylogenetic position of the "giant deer" *Megaloceros giganteus*. Nature 438, 850–853.
Maddison, W.P., Maddison, D.R., 2011. Mesquite: a modular system for evolutionary analysis. Version 2. 75. http://mesquiteproject.org.
Midford, P., Garland Jr., T., Maddison, W., 2011. PDAP Package of Mesquite. Version 1.16. http://mesquiteproject.org/pdap_mesquite/index.html.
Padian, K., Lamm, E.-T., 2013. Bone histology of fossil tetrapods: advancing methods, analysis, and interpretation. University of California Press, Berkley.
Peigné, S., Sen, S., 2012. Mammifères de Sansan, 203. Mem. Muséum National d'Histoire Naturelle, Paris.
Ponton, F., Elzanowski, A., Castanet, J., Chinsamy, A., Margerie, E., de Ricqlès, A., de Cubo, J., 2004. Variation of the outer circumferential layer in the limb bones of birds. Acta Ornithol. 39, 137–140.
Quemeneur, S., Buffrénil, V., de Laurin, M., 2013. Microanatomy of the amniote femur and inference of lifestyle in limbed vertebrates. Biol. J. Linn. Soc. 109, 644–655.
Solounias, N., Moelleken, S.M.C., 1994. Differences in diet between two archaic ruminant species from Sansan, France. Hist. Biol. 7, 203–220.
Stuart, A.J., Kosintsev, P.A., Higham, T.F.G., Lister, A.M., 2004. Pleistocene to Holocene extinction dynamics in giant deer and woolly mammoth. Nature 431, 684–689.
Van Der Geer, A.A.E., Lyras, G., de Vos, J., Dermitzakis, M., 2010. Evolution of Island Mammals. Adaptation and Extinction of Placental Mammals on Islands. Blackwell publishing, Chichester.
Vislobokova, I.A., 2013. Morphology, taxonomy, and phylogeny of megacerines (Megacerini, Cervidae, Artiodactyla). Paleontol. J. 47, 833–950.